Multispectral radiometer to measure crop canopy characteristics

E. J. Brach and P. Poirier

Engineering and Statistical Research Institute, Research Branch, Agriculture Canada, Ottawa, Ontario, Canada K1A 0C6

R. L. Desjardins

Land Resource Research Institute, Research Branch, Agriculture Canada, Ottawa, Ontario, Canada K1A 0C6

D. Lord

Department of Pathology, Laval University, St. Foy, Quebec, Canada G1V 2L9

(Received 2 September 1982; accepted for publication 6 November 1982)

A spectroradiometer has been designed for the study of crop reflectance characteristics in the spectral range of 400–1000 nm. Since the instrument records the ratio of incoming to reflected radiation the values obtained are independent of variations in solar elevation, and azimuth angle and atmospheric conditions. A filter wheel with four interchangeable interference filters is used for wavelength selection. The spectroradiometer traverses above a crop canopy on a movable track. This makes it possible to compare measurements from various locations several times in an hour, and to study more than one canopy a day. This instrument provides agronomists with data to estimate crop canopy characteristics such as leaf area index (LAI) rapidly and nondestructively. It also measures the variability of canopy reflectance introduced by temporal and spatial factors.

PACS numbers: 07.65.Eh, 07.65.Gj

INTRODUCTION

The physical and physiological base for the reflectance of solar radiation from plant leaves and canopies are known.[1,2] Scientists use reflectance measurements to deduce leaf parameters[3,4]; and crop canopy characteristics.[5–9] A variety of instruments have been developed to measure one of the numerous kinds of reflectance[10] or reflectance factors of a canopy.[11–16] The objective of this paper is to describe a spectroradiometer that measures the directional-conical reflectance of a crop canopy in order to develop techniques estimating its leaf area index (LAI) and its percentage ground cover (PGC). LAI, defined as the area of green leaves within a vertical cylinder of unit cross section,[17] is directly related to the reflectance of a canopy, whereas PGC, defined as the percentage of a unit of soil area covered by vegetation, is related to reflectance through its direct relation to LAI.[18] Both are used for estimating light interception and biomass productivity in crop yield modeling.[19–20]

In order to study spectral reflectance characteristics of crops for the same area for the whole growth cycle with a minimum manpower requirement, an instrument which corrects for variations in irradiance was developed. The spectroradiometer described measures almost simultaneously absolute values of incoming and reflected radiation in the spectral range 400–1000 nm. The reflectance of the crop is obtained from the ratio of reflected to incoming radiation for up to four different wavelengths.

I. INSTRUMENTATION DESIGN

The intensity and quality of the radiant energy $E_i(\lambda)$ falling on a crop canopy changes continuously. This is due to variation in atmospheric turbidity, cloud, and haze conditions as well as to continuous changes in solar elevation angle and the azimuth angle between sun, crop, and detector.[21] To neutralize this effect, the multispectral radiometer measures $E_i(\lambda)$ and $E_r(\lambda)$ the reflected radiation, in close proximity. The spectral values are ratioed to give the reflectance value R of the canopy

$$R = \frac{E_r(\lambda)}{E_i(\lambda)} \tag{1}$$

This instrument measures relative reflectance values but could be used to obtain absolute reflectance values with the use of known calibration targets.

The multispectral radiometer consists of optical, electronic, and mechanical sections. The optics of the system (Fig. 1) are designed to collect: (a) the incoming radiant energy; (b) the reflected energy from the crop.

The diffuser (d) along with the collimator (c) acts as a cosine corrected collector. It accepts all radiant flux from the hemisphere according to the cosine of the incident angle, as expressed by

$$E = I \cos \alpha \tag{2},$$

where $E =$ irradiance, $I =$ radiant intensity, and $\alpha =$ angle of incidence.

The diffuser is constructed from a white acrylic plastic (W2447, Kaufman Glass Co., Wilmington, Delaware) that attenuates the incoming radiant energy.

Figure 2 shows the percent error in the cosine response of the diffuser for light at four different wavelengths. Far red and near infrared to 900 nm, the cosine response is true up to 70 °. The diffuse radiant energy is guided through five light

 0034-6748/83/040493-08$01.30

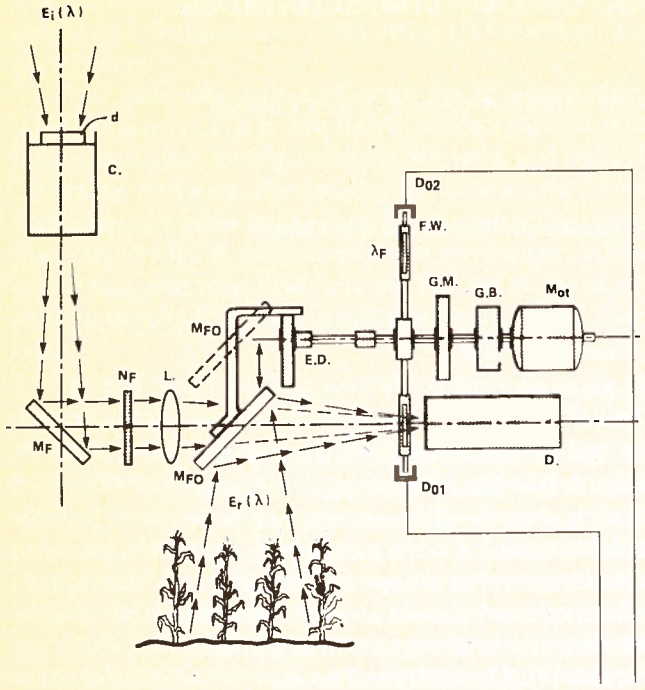

FIG. 1. Schematic diagram of optical and mechanical arrangements in the spectroradiometer.

tunnels which collimates the light onto a 1978-mm^2 45° flat mirror M_F.

In addition to the diffuser, a neutral density filter N_F (25%) is used to reduce $E_i(\lambda)$ to a magnitude close to $E_r(\lambda)$. The signal from the diffuser is directed to the detector by M_F and a 38-mm focal length lens (L) focuses the energy on to a 1-cm^2 silicon detector (D). The light beam is intercepted by one of the various interference filters (λ_F) placed on the filter wheel (Fw). The four interference filters of 25-mm diameter have the following center wavelength and half-bandwidth (HBW): λ_{F_1}, 647.6 nm (26.8 nm); λ_{F_2}, 675.5 nm (27 nm); λ_{F_3}, 739.9 nm (9.2 nm); λ_{F_4}, 790.4 nm (9.8 nm). The filters are interchangeable and any interference filter of 25-mm diameter and within the spectral range of the detector can be used. A folding mirror M_{FO} is placed at a 45° angle in the optical path of the radiant energy (Fig. 1). When M_{FO} is in the upward position, $E_i(\lambda)$ from M_F enters the detector through N_F, L, and λ_F. $E_r(\lambda)$ from the crop cannot reach the detector. When M_{FO} is in the downward position the path of $E_i(\lambda)$ is blocked and $E_r(\lambda)$ is directed by M_{FO} onto the detector. M_{FO} and the filter wheel are driven by a 3600-rpm, 60-Hz, hysteresis synchronous planetary gear reduced motor (Mot) with a speed reduction ratio of 36 (Globe Industries Inc., Dayton, Ohio). The gearbox (GB) output speed is 100 rpm, which is further reduced by 6.66:1 ratio producing 15 rpm. A geneva indexing mechanism (G.M.) is attached to the gearbox operating the filter wheel in an incremental mode of 3.75 rpm so that each interference filter is placed alternately in front of the detector for a period of 4 s. This period is divided into two equal parts by the change in the position of the M_{FO}, which is achieved by an eccentric drive (E.D.). E.D. is a cam attached to the filter wheel drive, which evenly divides the time of M_{FO} between its upward $E_i(\lambda)$ and downward $E_r(\lambda)$ position. Thus the time lapse between the measurement of $E_i(\lambda)$ and $E_r(\lambda)$ is 2 s which for practical purposes represents a simultaneous measurement.

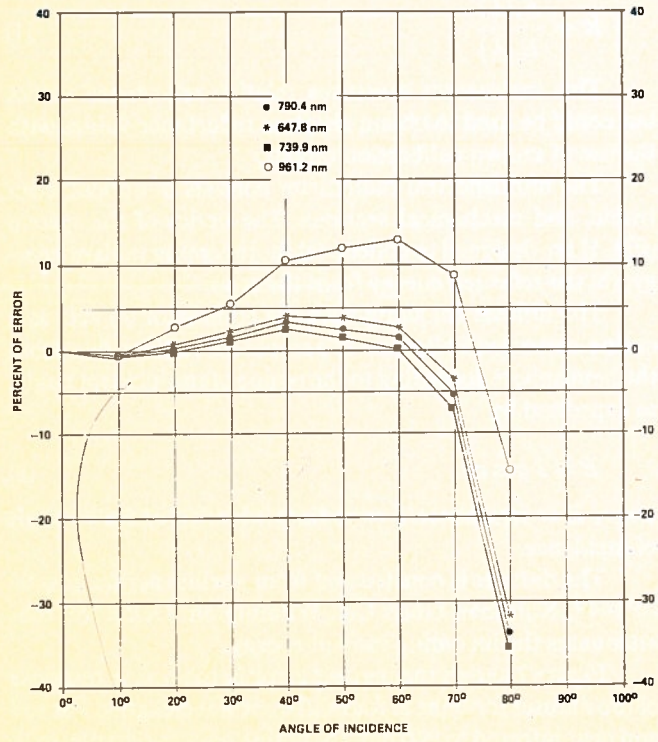

FIG. 2. The percentage error from the cosine response of the optical head for four interference filters.

A. Filter coding (Figs. 1 and 3)

To identify the filter placed before the detector, and to identify the start of a measuring cycle, a flange is secured to the center of each filter. The flange at filter λ_{F_1} is longer identifying the start of the cycle. The flanges pass through two optical detection assemblies (D_{01}, D_{02}), which are arranged so that only the larger flange passes through D_{01}, indicating the beginning of the cycle. The smaller flanges passing through D_{02} identify which filter is before the detector.

The optical detection assembly (GEH13B2, General Electric, Syracuse New York) combines a GaAs infrared emitting diode (D_1, D_2, Fig. 3), with a silicon photodarlington detector (Q_1, Q_4). Diodes D_1 and D_2 transmit light to phototransistors Q_1 and Q_2 across a 2.54-mm air gap as the flanges interrupt the light beam producing a signal at the outputs of the transistors. The pulse from Q_1 is 40 ms wide, and is shaped to its final form by transistors Q_2 and Q_3 (MPS6520) and associated circuits. This signal resets the data recording printer gating counter circuit C_1 (SN7490) through gates G_1 (SN7400) and G_{14} (SN7402) and triggers the paper advance through G_2 (SN7400). The pulse from Q_4 is 687 ms wide and is shaped to its final form by transistors Q_5 and Q_6 (MPS6520) and associated circuitry. For 687 ms through G_{14} this pulse keeps counter C_1 in reset and resets decimal counters C_4 and C_5 (SN7490) and multivibrator MU1 (SN7473).

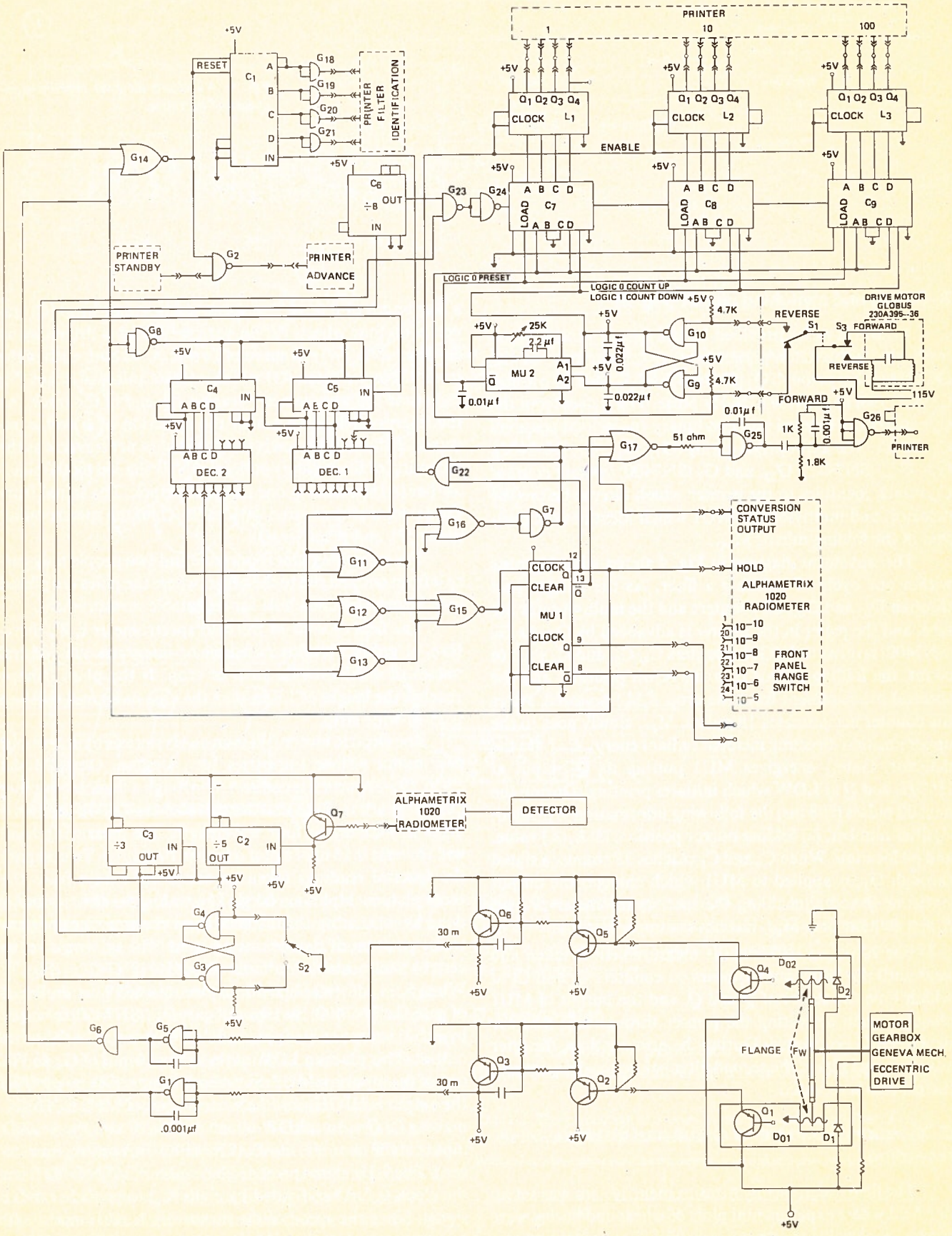

FIG. 3. Schematic diagram of filter coding, gating, and switching circuit.

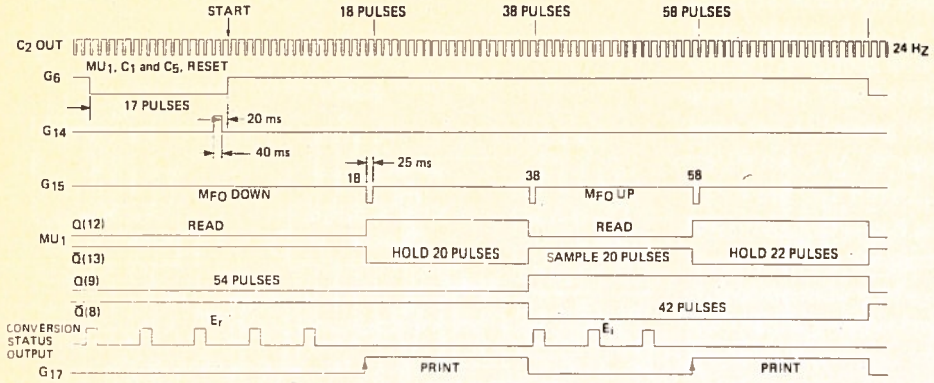

FIG. 4. Waveform diagram explaining sequence of operation.

B. Gating and switching circuit (Fig. 3)

A 120-Hz pulse provided by the system sample clock from the radiometer/photometer (Alphametrics Model DC1020) is fed through Q_7 (SN4401) and divided by counter C_2 (SN7490) to provide a 24-Hz pulse. The pulses from the C_2 counter are entered into two binary-to-decimal counters C_4 and C_5. The appropriate gating (G_{11}, G_{12}, G_{13} (SN7402), G_{15}, G_{16}, (SN7427), G_{22}, and G_7 (SN7400) operate counter C_1, which identifies to the printer which filter is before the detector, and multivibrator MU1 which identifies the position of the folding mirror M_{FO}.

The waveform diagram in Fig. 4 shows what happens within one cycle of indexing a filter. As the flanges pass through D_{01} and D_{02}, all counters and the multivibrator are reset and the paper in the printer is advanced by G_2. As G_6 (SN7400) returns to HIGH, counters C_4, C_5, and C_6 start to count, the folding mirror is in the down position, and the spectral measurement from the crop $E_r(\lambda)$ is stored. After the counter accumulates 18 pulses, M_{FO} slowly goes to the upper position directing incident radiant energy $E_i(\lambda)$ to the detector. $Gate_{15}$ energizes MU1 putting its $\bar{Q}$ output at HIGH, and Q at LOW which initiates printing. During the next 20 pulses (808 ms) the following information is printed: (1) filter number, (2) folding mirror position, (3) $E_r(\lambda)$ value, and (4) location. When C_4 and C_5 reaches 38 counts, a signal through G_{15} is applied to MU1 which changes the output status of Q and $\bar{Q}$ enabling the spectroradiometer to read $E_i(\lambda)$. By that time M_{FO} reaches the upper position.

For 20 pulses (808 ms) the measurement is taken and held until the 58th count appears on counters C_4 and C_5 at which time the status of Q and $\bar{Q}$, and the output of MU1 changes again activating the printer through G_{17} and the data for $E_i(\lambda)$ is printed. During the printing time, the filter advances and places the second filter before the detector and the process is repeated.

C. Measuring head travel circuit and distance recording

The field spectroscopy measurement system was set up in a field where experimental plots of wheat and barley were grown. A portable traversing unit (Fig. 5) supports and traverses the spectroradiometer. Four telescopic poles (K) are spaced 3.5 m apart. The height of the poles can be adjusted to a maximum of 3.6 m. The spectroradiometer head (C) traverses on four wheels (V) on a track (F) and is driven by an electric motor (W) at a speed of 10 mm/s. At both ends of the track there are stops (G) which operate microswitches (M) each time the spectrometer reaches the end of the track. As the microswitch is operated, the direction of travel is reversed. Diffuse radiation is measured once per traverse as the incoming radiant energy collector (N) is shaded by the shadow bar (A) attached at one end of the track. The signal from the detector is connected via a cable (O) to the spectroradiometer (P), and recorder (Q).

The traversing unit is portable and two people may carry it from one test site to the other, where the poles are placed into a predetermined hole for repeatable measurement.

The field of view of the field spectrometer is 8°, therefore, at ground level it measures or integrates the spectral values of a 0.5-m-wide strip of crop. If the plant canopy reaches the height of 1.8 m then the area measured will be a 0.25-m-wide strip.

The electric motor (W) is an ac Hysteresis Synchronous gear motor (Globe Industries Inc., Dayton, Ohio, Model 230A 395-36) which is connected through a flexible coupling (X) and gearbox (Z) to the four drive wheels (Y). In the 16 s it takes to measure at four wavelengths the measuring head will traverse 0.16 m of a plot which is 10 m long. To compare the spectral readings taken on consecutive days from the same plot, each plot is coded. The coding for this system is done by measuring the distance from the stop G of one extreme position of the measuring head. The system is set to zero by a monostable multivibrator MU2 (SN74121) (Fig. 3). When S_3 is in forward position, placing a LOW at the input of gate G_9 (SN7400) the input of gate G_{10} (SN7400) is biased by a 5-V source so its input is HIGH, giving a LOW to its output. This places a LOW at the second input of G_9 and to one of the inputs of MU2. Since both inputs of G_9 are LOW, the output is HIGH, and the second input of MU2 is HIGH, making its Q output LOW which is entered into the LOAD inputs of the counters C_7–C_9 (SN74190) thus setting them to zero. The 8-Hz signal provided by counter C_3 (SN7490) from the clock is further divided by eight (C_6) to provide a 1-Hz signal. Since the speed of the measuring head is exactly 10 mm per second, each 1-Hz signal represents 10 mm. When the main power switch S_1 and the microswitch S_3 for motor phase changes are in the "forward" position, the measuring

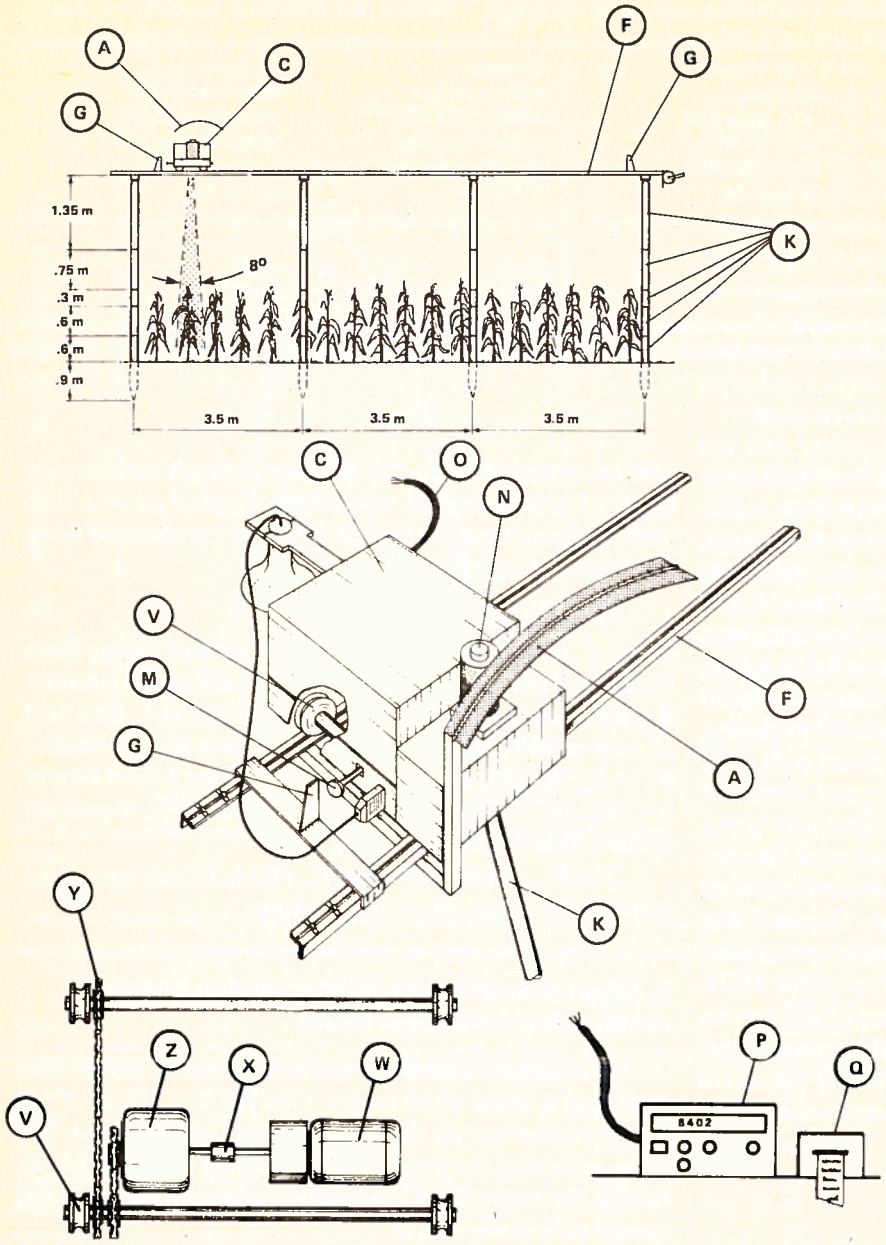

FIG. 5. Schematic diagram of portable traversing unit.

head moves forward, the 1-Hz signal enters the counter C_7 through gates G_{23} and G_{24} (SN7400). Every 2 s, when a radiant energy value is printed, the numbers on the counters C_7 to C_9 are latched or stored by latches L_1 to L_3 (SN7475). When the enable signal from gate G_7 is HIGH, the information present at a data input is transferred to the Q outputs, which is then printed. When S_3 is in the reverse position a LOW is placed at one of the inputs of gate G_{10}, the 5-V HIGH signal at the input at gate G_9 also energizes the A and D inputs of the counters C_7 to C_9 placing number nine in each counter, the HIGH from the output of gate G_{10} instructs the counters to count down from 999 to 0. The reading and printing of the data then follow the same process as the forward direction. If the measuring head is stopped at any position between the extremes of the traverse, the up/down counters are stopped with their numbers stored by their respective latches by a LOW signal at one of the inputs to gate G_4 which provides a LOW at the output of gate G_3 (SN7400) and in turn puts a LOW at the input at the gate of G_{23}, causing a HIGH at its output. Gate G_{24} inverts that to a LOW which stops the counts from counter C_6 from entering the up/down counter.

D. Radiometer

The radiometer (Alphametrics Model 1020) includes the probe and energy converter. The probe consists of a sili-

TABLE I. The percentage of overlap between measurements from λ_1 to λ_4 for the traversing spectroradiometer.

	λ_1	λ_2	λ_3	λ_4
λ_1	100	84	68	52
λ_2	84	100	84	68
λ_3	68	84	100	84
λ_4	52	68	84	100

TABLE II. Correlation coefficients between spectral reflectance data having their central wavelength in the same part of the electromagnetic spectrum.

Spectral region	All mean reflectance data of 1980 ($N^* = 404$)	All mean reflectance data taken on wheat canopy in 1980 ($N^* = 124$)	All mean reflectance data taken on 80.06.15 on three densities of a wheat canopy ($N^* = 23$)	All mean reflectance data taken on 80.06.25 on one density of a wheat canopy ($N^* = 7$)
Near infrared (λ_1 vs λ_2)	0.980	0.988	0.966	0.985
Red (λ_2 vs λ_4)	0.946	0.995	0.999	0.996

*N is the number of reflectance measurements used in the correlation analysis. Each of them is a mean of a 30-min sampling based on 26 to 32 individual measurements.

con photovoltaic detector and optical filters to smooth their spectral response. The spectral response is flat within $\pm 6\%$ from 400 to 1000 nm, with an absolute calibration accuracy of 5% and a sensitivity of 10^{-8} Wm^{-2}. The converter can accept a wide range of input currents from the detector, amplify this signal by a stable amplifier which functions as a current-to-voltage converter, and its output is fed to a low-pass amplifier. This signal is applied to an analog-to-digital converter where the analog signals are converted to binary-coded-decimal (BCD) signals and displayed on a $3\frac{1}{2}$-digit read out. The A/D converter contains several clocks of which one provides a 120-Hz signal for various gating and measuring functions. The radiometer also provides the conversion status output signal to gate G_{17} to instruct the printer to print the radiant energy data through G_{25} and G_{26} (SN7400). The auto range circuit of the radiometer is controlled by the Q and $\overline{Q}$ outputs from multivibrator MU1. Since the measurement of the incoming energy from the sun requires a different measuring range than the measurement of the reflected energy from the crop, the Q and $\overline{Q}$ output are connected to different range circuits (radiometer output terminals 1 and 20–24 covering from 10^{-5} to 10^{-10}).

E. Calibration

The multispectral spectroradiometer was calibrated using a calibrated 100-W quartz lamp with a temperature of 3200 K (Oriel Corp., Stamford, Connecticut).

The calibration was performed separately in each of the four filter positions, for both the incoming and reflected energy optical circuits.

The lamp was placed 0.5 m from the entrance of the incident $E_i(\lambda)$ and reflectance $E_r(\lambda)$ energies.

The aperture of $E_i(\lambda)$ and $E_r(\lambda)$ receive all the energy inside a solid angle of 180 ° and 8 °, respectively. These energies are transmitted to the detector through interference filters of known central wavelength $(\lambda_c)(\lambda_1,\lambda_2,\lambda_3,\lambda_4)$. The calibration constant for each of the filters are obtained using the following equation:

$$K_c = E_c.\Delta\lambda c/R_c, \tag{3}$$

where $E_c = E_{ic}$, or E_{rc}, the incoming radiant energy from the lamp given at wavelength λ_c; K_c = calibration constant K_{ic}, for reading $R_c = R_{ic}$ of the spectrometer at λ_c for a field of view of 180 °; K_c = calibration constant K_{rc} for reading $R_c = R_{rc}$ of the spectroradiometer at λc for a field of view of 8 °; and $\Delta\lambda_c$ = the wavelength band where the maximum transmission amplitude is 50%.

The K_{rc} values differ from K_{ic} (Table III) because of the constriction of the respective aperture.

F. Effect of spectroradiometer motion during measurement with four filters

It is obvious that if the spectroradiometer moves constantly at a speed of 10 mm/s, then the four filters of the spectroradiometer for the same cycle will not see exactly the same reflecting surface. When measuring from a 180-cm height, the radius (r) of the cone covering the area that the spectroradiometer sees is

$$r = h \tan\theta = 126 \text{ mm} \tag{4}$$

The spectroradiometer travels 40 mm between two consecutive reflected energy measurements (i.e., λ_1, λ_2). The center of the cone for each consecutive measurement thus differs by 40 mm in the direction of motion, which means that 16% of the reflected energy measured through two consecutive filters does not come from the same zone. This effect is even greater for nonconsecutive filters (i.e., λ_1, λ_4) as can be seen in Table I. However, if measurements are taken from

TABLE III. The calculated values of calibration factors K_{ic} and K_{rc} for four interference filters.

λ_c filter	$\Delta\lambda_c$ (nm)	$E_{ic} = E_{rc}$ (W cm^{-2} nm^{-1})	R_{ic} (10^{-10} W cm^{-2})	R_{rc} (10^{-7} W cm^{-2})	K_{ic}	K_{rc}
739.9	9.2	2.2	203	283	997	0.715
790.4	9.8	2.4	295	385	797	0.611
675.5	27.0	1.9	722	1131	711	0.454
647.6	26.8	1.7	528	864	863	0.527

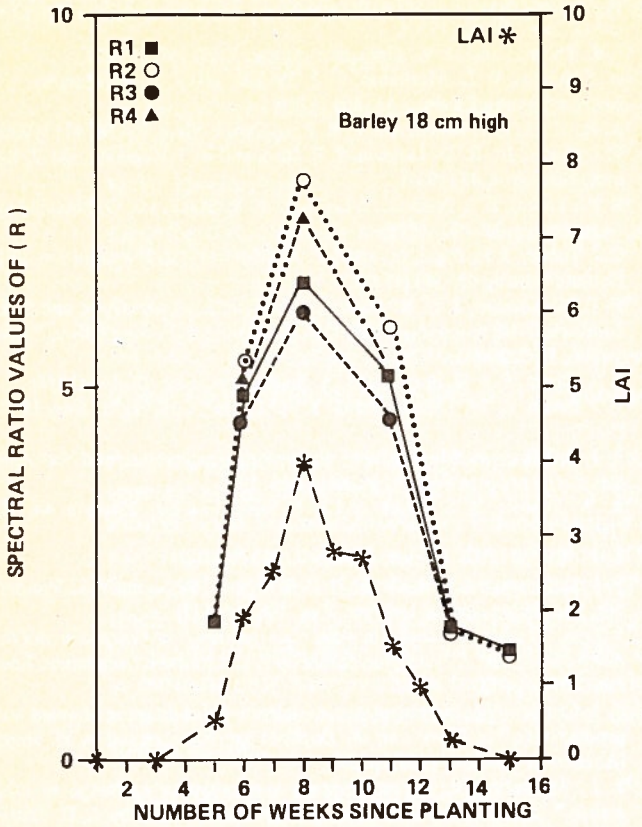

FIG. 6. Relationship between ratio values R_1 to R_4 in relation to leaf area index.

a height of 360 cm, these differences are reduced by half. This may introduce some errors, but since several measurements are taken from the same plot, the spectral readings may be averaged thus reducing the errors. Furthermore, the variability in measuring actual crop characteristics is much larger than the error introduced due to the sampling.

The high correlation coefficients between the spectral reflectances taken at two wavelengths from the same spectral region demonstrates that the effect of the motion of the spectroradiometer is corrected by the high sampling capability of the instrument (Table II). It indicates that an average of thirty reflectance measurements on one plot gives a mean reflectance value which is representative of the crop canopy.

Measurements: The reflected energy in the red (646.8 nm, 675.5 nm) and near infrared (739.9 nm, 790.4 nm) were compared with the LAI of a plant canopy. LAI measurements were taken weekly while reflectance measurements were generally obtained on sunny days. The period for reflectance measurements was always kept within 2 h of noon, which served to eliminate most of the effects of the solar elevation angle on the spectral reflectance.[22] Reflectance data were analyzed in the form of four ratios.

$$R_1 = \frac{(\lambda 4\uparrow/\lambda 4\downarrow)}{(\lambda 1\uparrow/\lambda 1\downarrow)}; \quad R_2 = \frac{(\lambda 4\uparrow/\lambda 4\downarrow)}{(\lambda 2\uparrow/\lambda 2\downarrow)};$$

$$R_3 = \frac{(\lambda 3\uparrow/\lambda 3\downarrow)}{(\lambda 1\uparrow/\lambda 1\downarrow)}; \quad R_4 = \frac{(\lambda 3\uparrow/\lambda 3\downarrow)}{(\lambda 2\uparrow/\lambda 2\downarrow)},$$

TABLE IV. Relationship of R_2 values and incoming radiant energy I_{r_2} to solar elevation angle.

Date	Time (hr)	Crop	Leaf area index	Solar elevation angle in °	R_2	I_{r_2}
05-06-80	10–11	barley	1.93	58	6.357	3.27
sunny,	11–12		1.93	60	5.789	3.20
slight	12–13		1.93	67	5.602	3.25
haze	13–14		1.93	68	5.334	3.21
17-06-80	10–11	barley	4.06	59	9.821	3.26
high,	11–12		4.06	61	8.527	3.23
cirrus	12–13		4.06	68	8.381	3.20
clouds	13–14		4.06	70	7.758	3.16
25-06-80	10–11	wheat	3.86	59	11.458	3.52
hot,	11–12		3.86	63	10.722	3.39
humid	12–13		3.86	68	10.069	3.40
	13–14		3.86	70	9.562	3.40
11-07-80	10–11	wheat	2.34	56	17.963	3.49
humid	11–12		2.34	61	12.671	3.54
	12–13		2.34	65	13.976	3.46
	13–14		2.34	68	12.608	3.59
24-07-80	10–11	barley	0.27	56	2.295	3.54
clear,	11–12		0.27	59	1.846	3.46
sunny	12–13		0.27	62	1.955	3.48
	13–14		0.27	66	1.841	3.46
25-07-80	10–11	wheat	1.09	55	9.003	3.59
sunny in	11–12		1.09	60	6.341	3.31
morning,	12–13		1.09	62	6.909	3.59
cloudy in afternoon	13–14		1.09	66	6.736	3.53
24-08-80	10–11	wheat	0.08	53	3.011	3.57
sunny	11–12		0.08	58	2.487	3.46
	12–13		0.08	60	2.519	3.51
	13–14		0.08	64	2.335	3.49

where the downward arrow (↓) indicates the incident radiant energy and the upward directed arrow (↑) the reflected radiant energy.

The mean ratio values of barley for 32 measurements taken are given in Fig. 6. The results indicate that the ratios follow each other closely up to the 8th week and from the 13th to the 16th week after seeding. But between the 7th and 12th week, the value for R_2 is higher than the other ratios. This suggests that R_2 ratios are the best wavelength to differentiate the green vegetative material. This result was expected from the physical and physiological basis of crop reflectance.[1]

To find the effect of the solar elevation angle on R_2, the measuring time was separated in four 1-h periods. Table IV shows R_2 and the incoming radiant energy I_{r_2} for wheat and barley at various growth stages. I_{r_2} is defined as the ratio of incident energy of wavelengths λ_2 and λ_4. The change in the incoming radiant energy I_r during the whole season did not change more than 12%. Within one day or between the four periods, the change varies by up to 3%. The variation of R_2 is up to 30% from the four periods, but the largest contribution to the variation is due to the data during the 10–11 h period from period one. When only the last three periods are taken into consideration, the variation in R_2 is around 8%.

ACKNOWLEDGMENTS

The authors wish to thank W. Reid and W. Fagan for their assistance in the design of the spectroradiometer mechanisms.

[1]E. B. Knipling, Remote Sensing Environ. **1**, 155, (1970).
[2]J. E. Colwell, Remote Sensing Environ. **3**, 175, (1974).
[3]H. W. Gausman, J. H. Everitt, and D. E. Escobar, J. Rio Grande Val. Hortic. Soc. **34**, 61 (1980).
[4]J. R. Thomas and H. W. Gausman, Agron. J. **69**, 799, (1977).
[5]D. S. Kimes, B. L. Markahm, C. J. Tucker, and J. E. McMurtrey, III, Remote Sensing Environ. **11**, 401 (1981).
[6]A. R. Mack, E. J. Brach, and V. R. Rao, Can. J. Plant Sci. **60**, 411 (1980).
[7]P. J. Pinter, Jr., R. D. Jackson, S. B. Idso, and R. J. Reginato, Int. J. Remote Sensing **2**, 43 (1981).
[8]R. W. Tinker, E. J. Brach, L. J. LaCroix, A. R. Mack, and G. Poushinksy, Agronomy J. **71**, 992 (1979).
[9]C. J. Tucker, J. H. Elgin, Jr., and J. E. McMurtrey, III, Photogramm. Eng. Remote Sensing **45**, 643 (1979).
[10]F. F. Nicodemus, J. C. Richmond, J. J. Heia, I. W. Ginsberg, and T. L. Limberis, NBS monograph 160, U.S. Government Printing Office, Washington, D.C. 20402, 1977.
[11]J. K. Berry, F. J. Heimes, and J. A. Smith, Opt. Eng. **17**, 143 (1978).
[12]E. J. Brach, R. W. Tinker, and G. T. St. Amour, Can. Agric. Eng. **19**, 78 (1977).
[13]E. J. Brach, A. R. Mack, and G. St. Amour, Engineering and Statistical Research Institute Report No. 6842-626, 1981.
[14]R. W. Leamer, V. I. Myers, and L. F. Silva, Rev. Sci. Instrum. **44**, 611 (1973).
[15]E. J. Milton, Int. J. Remote Sensing **1**, 153 (1980).
[16]B. F. Robinson, M. E. Bauer, D. P. DeWitt, L. F. Silva, and V. C. Vanderbilt, Soc. Photo-optical Instrum. Eng. **196**, 8 (1979).
[17]J. Ross, "Radiative transfer in plant communities," in *Vegetation and the Atmosphere, Vol. I, Principles*, edited by J. L. Monteith (Academic, London, 1976), p. 13.
[18]P. J. Curran, "Multispectral remote sensing for estimating biomass and productivity," in *Plants and the Daylight Spectrum*, edited by H. Smith (Academic, London, 1981), p. 55.
[19]J. L. Monteith, "Light interception and radiative exchange in crop stands," in *Physiological Aspects of Crop Yield*, edited by J. D. Eastin (American Society of Agronomy, Madison, WI, 1969), p. 89.
[20]W. G. Duncan, R. S. Loonie, W. A. Williams, and R. Hanan, Hilgardia **38**, 181 (1967).
[21]K. Ya. Kondratyev, *Radiation in the Atmosphere* (Academic, London, 1969), p. 912.
[22]R. D. Jackson, P. J. Pinter, Jr., R. J. Reginato, and S. B. Idso, USDA, Science and Education Administration, Agricultural Reviews and Manuals, ARM-W-1980.